

©2016

Xiangan Wang

ALL RIGHTS RESERVED

ASSESSING THE CYTOTOXICITY OF NEWLY DEVELOPED GLIADIN
NANOPARTICLES LOADING POLYMETHOXYFLAVONES

By

XIANGAN WANG

A thesis submitted to the

Graduate School-New Brunswick

Rutgers, The State University of New Jersey

In partial fulfillment of the requirements

For the degree of

Master of Science

Graduate Program in Food Science

Written under the direction of

Dr. Qingrong Huang

And approved by

New Brunswick, New Jersey

October 2016

ABSTRACT OF THE THESIS

Assessing the Cytotoxicity of Newly Developed Gliadin Nanoparticles Loading

Polymethoxyflavones

By XIANGAN WANG

Thesis Director:

Dr. Qingrong Huang

Whether the consumption of dietary supplements is helpful or not significantly depends on the bioavailability of the nutraceuticals. Since nutraceuticals dissolve poorly in aqueous system and undergo rapid and intensive metabolism, they are low in bioavailability. In this thesis, a novel delivery system was developed from gliadin to encapsulate polymethoxyflavones, and the cellular uptake and cytotoxicity of the system were assessed upon Caco-2 colon cancer cell lines.

Gliadin is the prolamin from wheat thus is GRAS (generally recognized as safe). The huge production of wheat domestic and oversea makes gliadin easily accessible. Gliadin is not well studied for its formulation of nanoparticles, let alone the physiochemical properties or cytotoxicity of gliadin particles. Polymethoxyflavones (PMF) are flavonoids from citrus peels. Although they have shown health benefits such as anti-cancer and anti-inflammation

effects, they are extremely low in bioavailability and hardly dissolve in water.

In the experiments, gliadin was extracted from commercial gluten, and its purity was evaluated before further study. The shape and size of 1 mg/ml gliadin in 60% ethyl-ethanol was shown prolate ellipsoid and 157 Å by 27 Å by 6 Å based on small angle X-ray scattering (SAXS). Preliminary trials were carried out to find out favorable conditions for gliadin nanoparticle formulation. The PMF-loaded gliadin nanoparticles were prepared by induced self-assembly. Particles presented spherical morphology shown by atomic force microscopy (AFM). Particles have a diameter around 150nm without any chemical agent to stabilize. The PMF-loaded gliadin nanoparticles demonstrated little, if there is any, cytotoxicity upon human colon cancer cells. In short, gliadin nanoparticles formulated in this study have reasonable loading and very low cytotoxicity and may be used to load lipophilic nutraceuticals other than PMF.

ACKNOWLEDGMENT

I would like to greatly thank my advisor, Dr. Qingrong Huang, for his kind and patient guidance and being so supportive to my Master's study in his research group. I've learned how to conduct research independently from Dr. Huang himself and his group. I am truly grateful to Dr. Huang for his training in instrumentation and his help in coursework.

I would also like to thank Dr. Chi-Tang Ho and Dr. Maria G. Corradini for kindly being my committee members and providing constructive advice and valued suggestions. In addition, I'd like to express my gratitude to all the faculty and staff in the Food Science Department at Rutgers University.

Also, my sincere thanks go to my lab mates; I've really enjoyed working with them and, more importantly, learning from them.

Lastly, I would like to thank my parents for their unconditional support both financially and emotionally.

TABLE OF CONTENTS

ABSTRACT OF THE THESIS.....	ii
ACKNOWLEDGEMENT.....	iv
TABLE OF CONTENTS.....	v
LIST OF TABLES.....	ix
LIST OF FIGURES	x
CHAPTER 1 INTRODUCTION.....	1
1.1 Nutraceuticals and Bioavailability	1
1.1.1 Nutraceuticals.....	1
1.1.2 Oral bioavailability.....	2
1.2 Nanoparticles in food science	3
1.2.1 Definition and potential of nanoparticles	3
1.2.2 Preparation of nanoparticles.....	3
1.3 Gliadin.....	5
1.3.1 Chemistry of gliadin, glutenin, and gluten	5
1.3.2 Current research on gliadin	8
1.4 Polymethoxyflavones: chemistry, benefits, and bioavailability	9
CHAPTER 2 OBJECTIVE.....	12
CHAPTER 3 EXTRACTION AND IDENTIFICATION OF GLIADIN FROM COMMERCIAL GLUTEN.....	13
3.1 Introduction.....	13

3.2 Materials and Methods.....	14
3.2.1 Materials.....	14
3.2.2 Extraction process	14
3.2.3 Nitrogen content measurement and FTIR spectroscopy	14
3.2.4 SDS-PAGE analysis	15
3.2.5 GPC analysis	15
3.3 Results and Discussion.....	16
3.3.1 Yield of gliadin from commercial gluten	16
3.3.2 Nitrogen content and FTIR results	16
3.3.3 SDS-PAGE Results	17
3.3.4 GPC Results	18
3.4 Conclusion	19
CHAPTER 4 STRUCTURE OF GLIADIN IN SOLUTION	20
4.1 Introduction.....	20
4.2 Experimental method	21
4.3 SAXS Results.....	21
4.4 Conclusion	26
CHAPTER 5 FORMULATION AND CHARACTERIZATION OF GLIADIN NANOPARTICLES	27
5.1 Introduction.....	27
5.2 Materials and method.....	28
5.2.1 Materials.....	28

5.2.2 Fabrication of gliadin nanoparticles	28
5.2.3 Hydrophobicity of gliadin	28
5.2.4 Formulation of PMF loaded gliadin particles.....	29
5.2.5 Morphological study by Atomic Force Microscopy (AFM)	29
5.2.6 Particle size distribution and ζ -potential measurement	29
5.2.7 PMF loading and encapsulation efficiency in gliadin particles.....	30
5.3 Results and discussion	31
5.3.1 Optimum condition for gliadin nanoparticle formation	31
5.3.2 Hydrophobicity of gliadin	33
5.3.3 Morphology of PMF-loaded gliadin particle: AFM results.....	34
5.3.4 Physicochemical evaluation of gliadin nanoparticles.....	35
5.4 Conclusion	36
CHAPTER 6 CYTOTOXICITY OF GLIADIN PARTICLE FORMULATION AND ITS CELLULAR UPTAKE PROFILE	38
6.1 Introduction.....	38
6.2 Materials and methods	38
6.2.1 Materials.....	38
6.2.2 Cytotoxicity of raw PMFs, blank gliadin particles, and PMF-loaded particles	39
6.2.3 Statistical analysis	40
6.2.4 Cellular uptake study on PMF-loaded gliadin nanoparticles.....	40
6.3 Results and discussion	41
6.3.1 Cell viability of raw PMFs, blank gliadin particles, and PMF-loaded gliadin particles	

.....	41
6.3.2 Cellular uptake profile of final formulation	44
6.4 Conclusion	48
REFERENCES.....	49

LIST OF TABLES

Table 1.1 Sub-types of gliadin: molecular weight and proportions in gluten.....	6
Table 1.2 Structure and molecular weight (MW) of major PMFs.....	11
Table 5.1 Trials of solvent vs. anti-solvent (Ratio v/v), gliadin concentration ([c] of gliadin), and presence of CMCS on particle size	32
Table 5.2 Physicochemical properties of gliadin nanoparticles	36

LIST OF FIGURES

Figure 1.1 Annual sales and expected trend of dietary supplements in the U.S.	2
Figure 1.2 Illustration of glutenin macromolecule structure (Don, Lichtendonk, Plijter, & Hamer, 2003)	7
Figure 3.1 FTIR spectrum of gliadin extract.....	17
Figure 3.2 SDS-PAGE data for gliadin extract	18
Figure 3.3 GPC data of gliadin extract.....	19
Figure 4.1 Intensity profile of 1mg/mL gliadin in 60% aqueous ethanol solution.....	23
Figure 4.2 GNOM fitting for experimental data against model of rod	24
Figure 4.3 GNOM fitting for experimental data against model of globular	25
Figure 4.4 GNOM fitting for experimental data against model of prolate ellipsoid	26
Figure 5.1 Water-in-air contact angle of gliadin film by VCA optima setup	33
Figure 5.2 Height image of blank (left) and loaded (right) nanoparticles by AFM	34
Figure 5.3 3-D image of blank (left) and loaded (right) nanoparticles by AFM	35
Figure 5.4 Direct observation of blank(left) and loaded (right) gliadin nanoparticles.....	36
Figure 6.1 Cell viability of Caco-2 cells treated with PMF in DMSO.....	42
Figure 6.2 Cell viability of Caco-2 cells treated with a series dilution	43
Figure 6.3 Cell viability of Caco-2 cells treated with PMF in DMSO and PMF-loaded	44
Figure 6.4 Cellular uptake of final formulation: fluorescence	47

CHAPTER 1 INTRODUCTION

1.1 Nutraceuticals and Bioavailability

1.1.1 Nutraceuticals

Nutraceutical is combined from “nutrition” and “pharmaceutical”, first introduced by Stephen L. DeFelice, founder and chairman of the Foundation of Innovation Medicine, in 1989 (Kalra, 2003). The concept of “nutraceutical” is fresh-born, and refers to the bioactive compounds that has physiological benefits and may protect consumers from chronic diseases, such as cancer, diabetes, and cardiovascular diseases (Kalra, 2003). Dietary supplements and functional food are examples of nutraceutical products on the market. Apparently, the general public cares about health; Mintel report has demonstrated a steady growth of the sales of dietary supplements since 2009 shown in Figure 1.1 (Mintel, 2014).

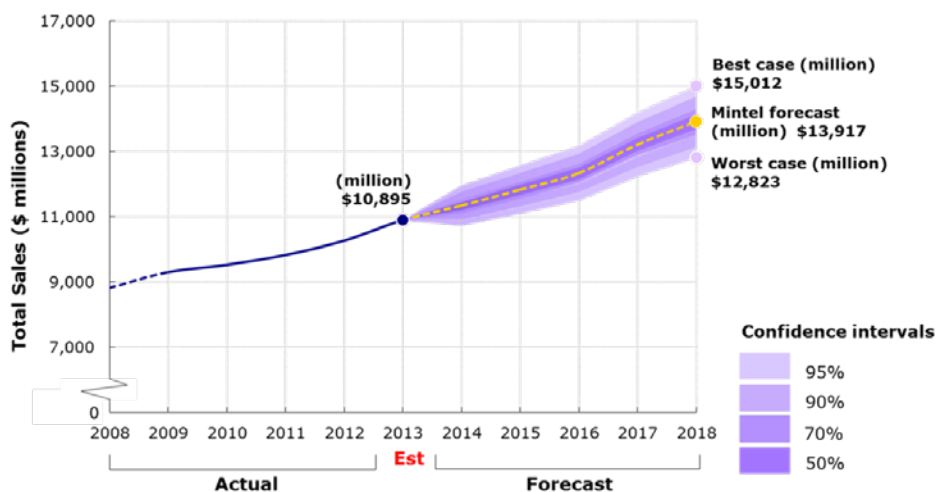


Figure 1.1 Sales and expected trend of dietary supplements in the U.S. (Mintel, 2014)

1.1.2 Oral bioavailability

Despite of the promising market, the consumed nutraceuticals do not necessarily contribute to health significantly. Whether or not the dietary supplements are helpful largely depends on the bioavailability of nutraceuticals. Unfortunately, most nutraceuticals are of low oral bioavailability, although oral delivery is non-invasive and commonly accepted.

For a given nutraceutical, oral bioavailability describes the amount in the blood circulation when it's taken by oral delivery, or eating (Pintore, Piclin, Chrétien, & Van De Waterbeemd, 2003). Internally, bioavailability is determined by ADME- absorption, distribution, metabolism, and excretion (Damodaran, Parkin, & Fennema, 2007). Therefore, anything that influences ADME contributes to bioavailability indirectly. Examples would include but are not limited to chemical properties and metabolic fates of nutrient.

Various factors lead to the low bioavailability of nutraceuticals. First of all, nutraceuticals dissolve poorly in aqueous system, thus are vulnerable to quick elimination from the gastrointestinal tract (Bell, 2001; Loveday & Singh, 2008). In addition, most nutraceuticals are polar to lipophilic cell membranes and have low mucosal permeability and cellular uptake (Bell, 2001; Galindo-Rodriguez, Allemann, Fessi, & Doelker, 2005). Consequently, those limitations restrict the effectiveness and health benefits of oral-taken dietary supplements.

1.2 Nanoparticles in food science

1.2.1 Definition and potential of nanoparticles

To address the issue of low bioavailability, nanoparticle is a highly potential solution. Nanoparticles are colloidal carriers scaled around 100 nm. Blank nanoparticles are made from natural polymers such as proteins and combinations of proteins and polysaccharides. Nanoparticles loaded with target compounds are categorized as nanocapsules and nanospheres; the former have core/shell structure while the latter a uniform matrix structure (Couvreur, Dubernet, & Puisieux, 1995). By loading target compound with nanoparticles, hydrophobic nutraceuticals can be dispersed in aqueous system evenly, perform controlled release, and enhance the uptake through the epithelial lining (Galindo-Rodriguez, Allemann, Fessi, & Doelker, 2005; Lamprecht, Saumet, Roux & Benoit, 2004).

Edible nanoparticles are readily to be applied in functional food or dietary supplements. For example, they may be fortified into beverage or dressing in their native form as long as they are stable at low pH. After freeze-dried, nanoparticles could be carried in capsules or tablets as dietary supplements.

1.2.2 Preparation of nanoparticles

More often than not, nanoparticles in food science are prepared by “bottom-up” approach, where nanoparticles are prepared by electrostatic interactions or anti-solvent induced self-

assembly. To form edible nanoparticles, proteins are of great importance. As proteins, the presence of multifunctional group makes interaction with nutraceuticals possible (Elzoghby, Abo El-Fotoh, &Elgindy, 2011). Also, proteins can provide biological support for nutraceuticals ((Ezpeleta, Irache, Stainmesse, Chabenat, Gueguen, Popineau, &Orecchioni, 1996). Most importantly, protein is GRAS (generally recognized as safe) and can be applied in the food industry.

After partial denature and/or gelation, water-soluble proteins (gelatin, collagen, casein, legumin, etc.) are capable of forming nanoparticles with calcium ions or charged polysaccharides. Electrostatic interactions of proteins happen when pH is away from their isoelectric points, and contribute to nanoparticle formation. However, their hydrophilic nature leaves water-soluble proteins vulnerable to enzymatic degradation; sometimes nanoparticles made from water-soluble proteins require non-food-grade cross-linkers to stabilize (Muzzarelli, 2009).

In contrast, prolamins usually do not need further modification or chemical cross-linkers to form nanoparticles. Prolamins are plant proteins that are insoluble in water and soluble in aqueous ethanol. Self-assembly happens when prolamin-in-ethanol solution is added into a large amount of anti-solvent (usually water) and the solubility of prolamins drops dramatically. The formation of nanoparticles and encapsulation of nutraceutical take place simultaneously. Prolamins then self-assemble into nanoparticles that repel each other due

to electrostatic force. Such process may be industrialized owing to its simplicity.

1.3 Gliadin

1.3.1 Chemistry of gliadin, glutenin, and gluten

Gliadin is a group of prolamins from wheat berry. Wheat is one of the predominant cereal grains of all times. In 2008, wheat production ranked fourth among all commodities produced worldwide (FAOSTAT, 2011). Cereal-seed proteins can be categorized based on the Osborne's sequential extraction (Osborne, 1907). Albumins (extractable with water) and globulins (extractable in salt solutions) are non-gluten-forming proteins, which takes 15% to 20% of total wheat proteins (Wieser, Antes, & Seilmeier, 1998). Gluten proteins are predominating in wheat proteins, occupying more than 75% (Delcour, Joye, Pareyt, Wilderjans, Brijs, & Lagrain, 2012). "Gluten" is often interchangeable with "gluten proteins", which is the viscoelastic, rubbery mass obtained by thoroughly washed wheat dough (Wieser, 2007). Gluten proteins are hardly extractable with water or salt solution, and can be further classified as gliadin and glutenin (Wieser, 2007).

Although both belongs to gluten proteins, gliadin differs from glutenin in several differently ways. Gliadin takes more than half of total gluten proteins, 58%-77% to be more specific (Wieser, 2007). Gliadins are monomeric and have average molecular weight between 28 to 55 kDa, whereas glutenins are polymers with much higher molecular weight

from 80kDa to more than 1000kDa (Tatham, Masson, & Popineau, 1990). Besides, gliadin has higher proline and phenylalanine composition but lower glycerin than glutenin (Wieser, 2007).

The hydrophobicity and relatively low molecular weight contributes to the good solubility of gliadin in aqueous ethanol. Gliadins can be further classified into four sub-types based on amino acid sequences and compositions, ω 5-, ω 1, 2-, β/α -, and γ -gliadin (Wieser, Antes, & Seilmeier, 1998). Sub-types of gliadins differ in molecular weight and proportions in gluten, as demonstrated in Table 1 (Wieser, 2007). It's worth mentioning that α -gliadins are responsible for the allergic reactions (Kobrehel, Bois, & Falmet, 1991). The secondary structure of gliadin has an overall compact globular structure; and gliadin has different number of intra-molecular disulfide bonds among sub-types (Veraverbeke & Delcour, 2002).

Table 1.1 Sub-types of gliadin: molecular weight and proportions in gluten (Wieser, 2007).

Type	MW (kDa)	Proportions (%)
ω 5-gliadins	49-55	3-6
ω 1, 2-gliadins	39-44	4-7
β/α -gliadins	28-35	28-33
γ -gliadins	31-35	23-31

On the other hand, glutenin is insoluble in most solvents (including acetic acids) due to its extraordinary molecular weight. Although the exact structure of glutenin is not known for sure, the most popular brief states that glutenins are composed of a linear backbone (high molecular weight glutenin subunits, or HMW-GS) and one or more braches (low molecular weight glutenin subunits, or LMW-GS) (Singh, & MacRitchie, 2001). The large backbone and relatively small braches are linked through inter-molecular disulfide bonds. Treated with reducing agents, inter-molecular disulfide bonds break, and LMW-GS are dismissed from backbone (Don, Lichtendonk, Plijter, & Hamer, 2003). Those free LMW-GS demonstrates similar solubility with gliadins (2003).

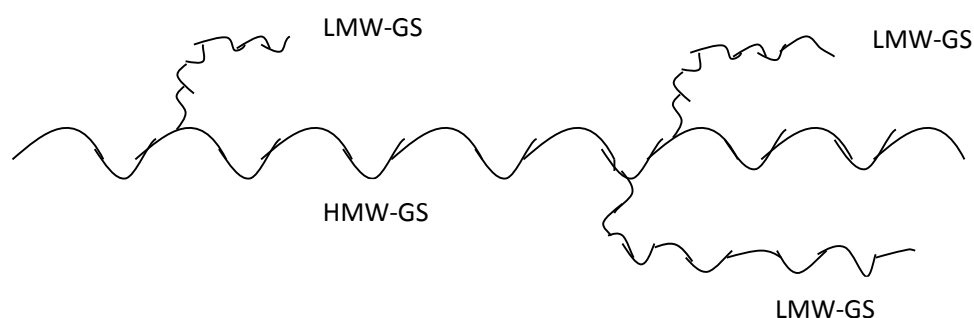


Figure 1.2 Illustration of glutenin macromolecule structure (Don, Lichtendonk, Plijter, & Hamer, 2003)

To put all in a nutshell, the hydrophobicity and high proportion of gliadin in wheat berry makes it suitable for nanoparticle formulation via self-assembly. Gliadins can be further classified into four sub-types, with various molecular weight from 28 kDa to 55 kDa.

Moreover, the abundance of wheat production annually domestic and oversea means easy access towards raw material. Distinct chemical properties of gluten proteins justify the extraction and separation of gliadin from commercial gluten using aqueous ethanol.

1.3.2 Current research on gliadin

Present academic study on gliadin focuses on its functionality in bakery products and dough formation, since flour or gluten is staple food in most countries. Some studies were conducted on the application of gliadin in terms of film formation to achieve controlled-release food package. Gliadin film has been well studied, including but not limited to favorable conditions for gliadin film formation, its sensitivity towards humidity and physical force, and its application as edible food package. Most studies suggest gliadin film is more vulnerable to humidity than pressure (Kieffer, Schurer, Köhler, & Wieser, 2007; Balaguer, Cerisuelo, Gavara, & Hernandez-Muñoz, 2013), with a reasonable tolerance to normal force but not shear force (Koehler, Kieffer, & Wieser, 2010).

Meanwhile, not much research has yet been dedicated to gliadin nanoparticles. With related publication scattered, the understanding towards gliadin nanoparticles are largely limited. A recent study on gliadin nanoparticles developed a formulation of blank gliadin particles and investigated the stability upon various temperature and pH (Joye, Nelis, & McClements, 2015). The reported formulation, however, was not defined at all because the

authors diluted gliadin extract instead of preparing gliadin solutions. In other words, others cannot reproduce or accommodate their formulation, because the concentration of gliadin solution is unknown.

So far it's been confirmed that gliadin nanoparticles are more stable when loaded with non-polar nutraceuticals than polar nutraceuticals (Duclairoir, Orecchioni, Depraetere, & Nakache, 2003). The controlled release profile was reported similar to zein-based nanoparticles, demonstrating a burst release within one hour followed by a gradual release later on (Duclairoir, Orecchioni, Depraetere, & Nakache, 2002). On the other hand, little has been revealed on the morphology or cytotoxicity of gliadin nanoparticles. Information that indicates the shape and size of gliadin in aqueous ethanol is also absent.

1.4 Polymethoxyflavones: chemistry, benefits, and bioavailability

Polymethoxyflavones (PMFs) are flavonoids almost exclusively from citrus peel. PMFs used in this thesis were extracted from bitter orange peel by column chromatography in previous study. PMFs possess multiple methoxyl groups on 15-carbon benzo- γ -pyrone skeleton (C6-C3-C6) with a C4 carbonyl group, in each molecular. PMFs differ from each other due to varied number/position of methoxyl groups. There have been more than twenty distinct PMF isolated and identified, among which tangeretin and nobiletin are most common and abundant (Li, Lambros, Wang, Goodnow, & Ho, 2007).

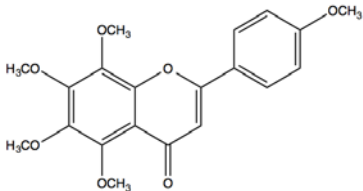
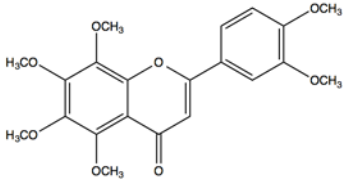
Commercial citrus commodities include oranges, lemons, and grapefruit. The annual production of citrus fruits is approximately 10 million tons, thus yields large amount of citrus peel as byproduct by beverage industry (Ting, Xia, Li, Ho, & Huang, 2013). The utilization of PMFs from otherwise discarded citrus peel creates additional economic value to the society.

PMFs are emerging bioactive compounds that have demonstrated various health benefits by a great number of publications. So far, PMFs have shown multiple biological activities, such as anti-inflammatory (Ho, Pan, Lai, & Li, 2012), anti-atherosclerosis (Li, Pan, Lo, Tan, Wang, & Shahidi, 2009), and anti-tumor (Miyata, Sato, Imada, Dobashi, Yano, & Ito, 2008). Particularly, tangeretin were documented to exhibit selective anti-proliferative activity towards cancer cells while sparing normal cells (Stoner, Kaighn, Reddel, Resau, Bowman, & Naito, 1991) and cholesterol-lowering effect (Kurowska & Manthey, 2004).

Unfortunately, such great biological value is greatly limited by low bioavailability. Compared with polyhydroxylated flavonoids, PMFs are more lipophilic, as methoxyl group are more hydrophobic than hydroxyl group. That is to say, PMFs are easier to pass through small intestine (Kurowska & Manthey, 2004). Even so, PMFs still have low bioavailability, because they poorly dissolve in water and undergo rapid and extensive metabolism after consumption (Nielsen, Breinholt, Cornett, & Dragsted, 2000).

In this thesis, PMF is the nutraceutical loaded in the gliadin nanoparticles. PMFs are white crystalline in room temperature and are stable at ambient and slightly elevated temperature (up to 80 degrees centigrade). Therefore, PMFs are easily accepted in the research and on the market. The molecular weight of PMFs falls in the range as can be encapsulated in nanoparticles.

Table 1.2 Structure and molecular weight (MW) of major PMFs

Name	Structure	MW (g/mol)
Tanngeretin (5,6,7,8,4'-penta methoxyflavone)		372
Nobiletin (5,6,7,8,3',4'-hexa methoxyflavone)		402

CHAPTER 2 OBJECTIVE

The objective of this thesis is to partially fill in the blanks of gliadin nanoparticle study. To better understand gliadin as a protein, its shape and size was briefly examined in SAXS. It is of great interest to study how gliadin nanoparticles could disperse PMFs in aqueous system and affect on human cells in terms of cytotoxicity and uptake. Therefore, the PMF-loaded gliadin nanoparticles were formulated, characterized, and evaluated on cell culture.

First, the favorable conditions for gliadin particle formation were investigated with a refined formulation finalized. Second, the blank formulation was used to load PMF; the characteristics of the loaded gliadin nanoparticles were studied. Last, both blank and loaded formulation were tested upon Caco-2 human cancer cells for cytotoxicity.

Overall, it would be better understood of the eligibility and capability of gliadin nanoparticles being adequate nutraceutical carrier.

CHAPTER 3 EXTRACTION AND IDENTIFICATION OF GLIADIN FROM COMMERCIAL GLUTEN

3.1 Introduction

Gliadin is the ethanol-soluble portion of gluten proteins. Gliadin is a complex combination of wheat proteins that share similar amino acid profile and can be further divided into four sub-types, ω 5-, ω 1, 2-, β/α -, and γ -gliadin. The molecular weight of gliadin varies between 28 to 55 kDa.

Gliadin and glutenin can be differentiated by their solubility in aqueous ethanol. Glutenin proteins have such high molecular weight (100 kDa or higher) that they hardly dissolve in most solvent. In addition to the difference in solubility, the amino acid profile of glutenin units differ from gliadin. Commercial gluten is mostly gluten proteins with very low amount of carbohydrates and little lipids. Therefore, gliadin is extracted by aqueous ethanol and separated through centrifugation.

To ensure the purity of the extracted gliadin is adequate for nanoparticle formulation, a series of identification test were conducted. The chemical identify was confirmed with Fourier Transform Infrared Spectroscopy (FTIR). The protein content (on a wet basis) was examined by Kjeldahl method, along with moisture content analysis. The molecular weight

was confirmed by sodium dodecylsulphate-polyacrylamide gel electrophoresis (SDS-PAGE) and gel permeation chromatography (GPC).

3.2 Materials and Methods

3.2.1 Materials

Gliadin was extracted from commercial gluten (Vital Wheat Gluten) purchased from Arrowhead Mills. Water purified by the Milli Q system was used throughout the experiments except for GPC assay, where water (HPLC grade) was purchased from Pharmco-AAPER (Brookfield, CT, USA). Na_2HPO_4 (ACS grade), NaH_2PO_4 (ACS grade), and sodium dodecylsulphate (ACS grade) were purchased from Sigma-Aldrich. 70% and 60% ethyl-ethanol were prepared using 95% ethyl-ethanol (ACS grade) from Pharmco-AAPER.

3.2.2 Extraction process

Gliadin was purified from lipid-free commercial gluten by Arrowhead Mills. The extraction process is adopted and modified based on previous studies (Wang, Tao, Wu, Yang, Chen, Jin, & Xu, 2014; Joye et al., 2015). Briefly, 20g commercial gluten was extracted twice with 200ml 70% ethyl-ethanol under mechanical stirring for 2 h, followed by centrifugation at 10,000g for 20 min. Between two extracting process, the cohesive mixture was chopped to pieces using spatula. The ethanol in supernatants was removed by

rotary evaporation at 30 °C. The gliadin extraction was freeze-dried and ground to make light yellow powder for use.

3.2.3 Nitrogen content measurement and FTIR spectroscopy

To estimate the protein content in the gliadin extraction, the nitrogen content (on wet basis) was examined by Kjeldahl method. The moisture content of gliadin extract was determined by Denver Moisture Analyzer IR-200 (Denver Instrument, Bohemia, NY). FTIR spectrum was obtained from Nicolet-Nexus 670 FTIR spectrometer (Fisher Scientific Inc., MA, USA). Gliadin extract was examined 128 scans with 4cm^{-1} resolution between 4000 to 600cm^{-1} for each measurement. Spectrum was exported by OMNIC 7.2 software.

3.2.4 SDS-PAGE analysis

The molecular weight distribution of gliadin extract was estimated by SDS-PAGE. Classic Laemmli buffer system was used as running buffer. The gliadin sample was suspended in the sample buffer at 2.5 mg/ml and 5mg/ml, respectively. 161-0318 Prestained SDS-PAGE Standards (Bio-Rad Laboratories, Hercules, CA) were used as protein molecular weight standards. After the sample was heated in boiling water for 10 min, the solution was used for SDS-PAGE analysis (Bio-Rad Laboratories, Hercules, CA) and separated in a 1mm thick preparative gel containing 12 % of resolving gel and 4% of stacking gel. Runs were performed at 80V.

3.2.5 GPC analysis

The protein size distribution was tested by GPC on a high performance liquid chromatography (HPLC) from Dionex (Sunnyvale, CA, USA) with an UltiMate 3000 Pump. Separation was performed on Acclaim® PolarAdvantage HPLC column (3 X 250mm, 3µm), and the collection of data was achieved by Chromeleon software. Ultraviolet detector (UltiMate 3000 Variable Wavelength) was used to detect gluten proteins at 214 nm wavelength.

Conditions for GPC analysis was adopted from previous study (Lagrain, Brijs, Veraverbeke, & Delcour, 2005). The mobile phase was 0.05M sodium phosphate buffer of pH 6.8 with 0.2% SDS. Gluten proteins were dissolved in 2% SDS in 0.05M phosphate buffer (pH 6.8) at 2mg/ml. The sample was then eluted at a flow rate of 0.7 mL/min for 25 min.

3.3 Results and Discussion

3.3.1 Yield of gliadin from commercial gluten

In this study, gliadin extract was from commercial gluten based on its good solubility in aqueous ethanol. The yield was 23.0% by weight, meaning that approximately every 100g commercial gluten gives 20-25g of gliadin. The extraction process doesn't have to start over from Osborne's sequential method, as commercial gluten is handily accessible in the market. Overall, the extraction of gliadin is simple and productive.

3.3.2 Nitrogen content and FTIR results

Protein content was estimated 88.2% based on nitrogen content on wet basis. Meanwhile, the moisture content was 8.65%, indicating a little bound water. Given that, the protein content was more than 95% on dry basis.

The IR spectrum confirms the sample protein (Figure 3.1). The absorbance from 3271-3390 cm^{-1} indicates N-H stretching vibration and/or -OH, and the most intense peak around 1645 cm^{-1} presents C=O and C-N groups. Another characteristic protein peak was near 1530 cm^{-1} , which was the combined effects of N-H, C-N and the C-C stretching vibrations. Absorbance near 3000-3200 cm^{-1} are truly indicative of -CH₃ and -CH₂- groups.

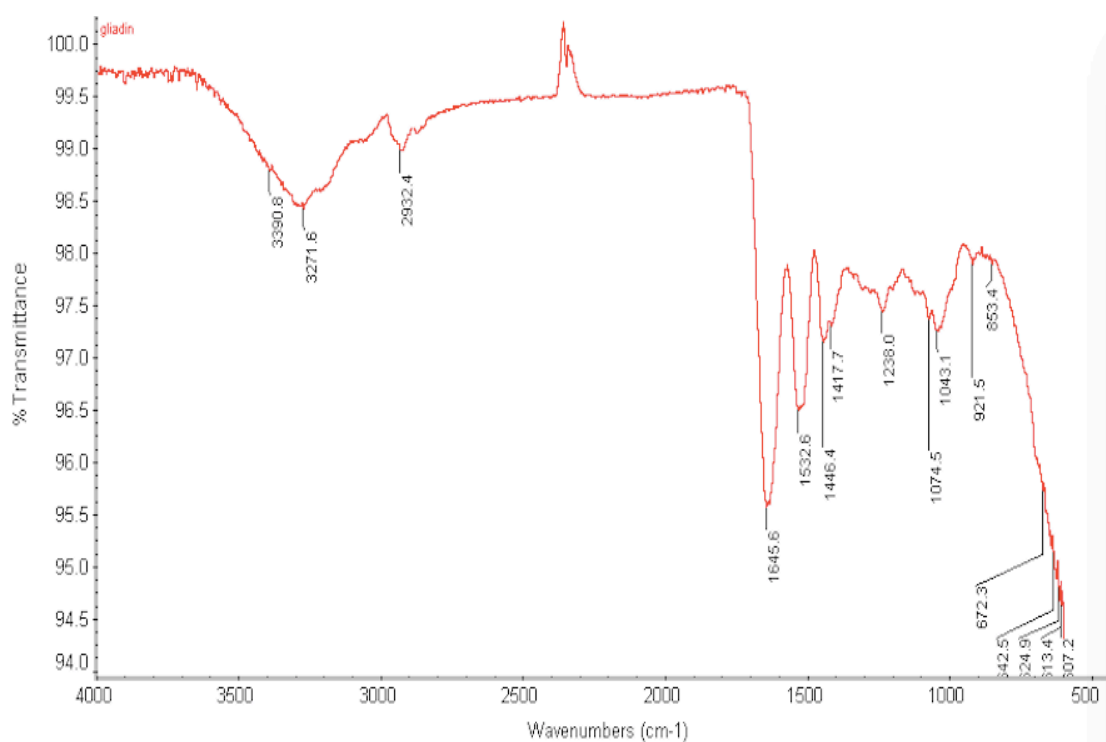


Figure 3.1 FTIR spectrum of gliadin extract

3.3.3 SDS-PAGE Results

SDS-PAGE reveals molecular weight of gliadin extract (Figure 3.2). The intensity and distribution of protein bands were similar with the data previously reported (Dahesh, Banc, Duri, Morel, & Ramos, 2014). In Figure 3.2, two major bands were identified between 25kDa and 55kDa, with the upper band being ω -gliadins, since ω -gliadins have highest average molecular weight. The lower band were highly likely α/β - and γ -gliadins; those three sub-types share similar molecular weight. The absence of any band above 55kDa suggested little amount of high molecular glutenin units.

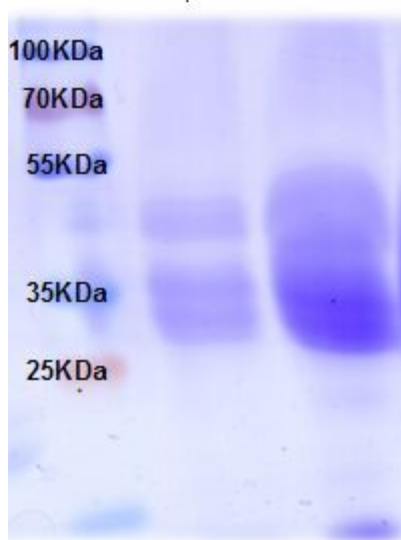


Figure 3.2 SDS-PAGE data for gliadin extract

3.3.4 GPC Results

GPC results (Figure 3.3) and SDS-PAGE results were alike. Two significantly overlapped

constituents were eluted at 9 min and 10.5 min. A minor tail peak showed at 12 min, almost covered by the 10.5 min peak. Based on the molecular weight of different sub-type gliadins, 9 min peak was two ω -gliadins (ω 5- and ω 1,2-). Since α/β -gliadins have slightly lower average molecular weight than γ -gliadins, 10.5 min peak was a combination of α/β - and γ -gliadins. Due to the high composition of α/β -gliadins, it was totally reasonable to have minor tail peak at 12 min. It's worth mentioning that gliadins used to classified as α -, β -, γ -, and ω -gliadin sub-types when scientists hadn't acquired sufficient understanding over their primary structure. Now gliadins have been re-categorized as ω 5-, ω 1,2-, α/β -, and γ -gliadins.

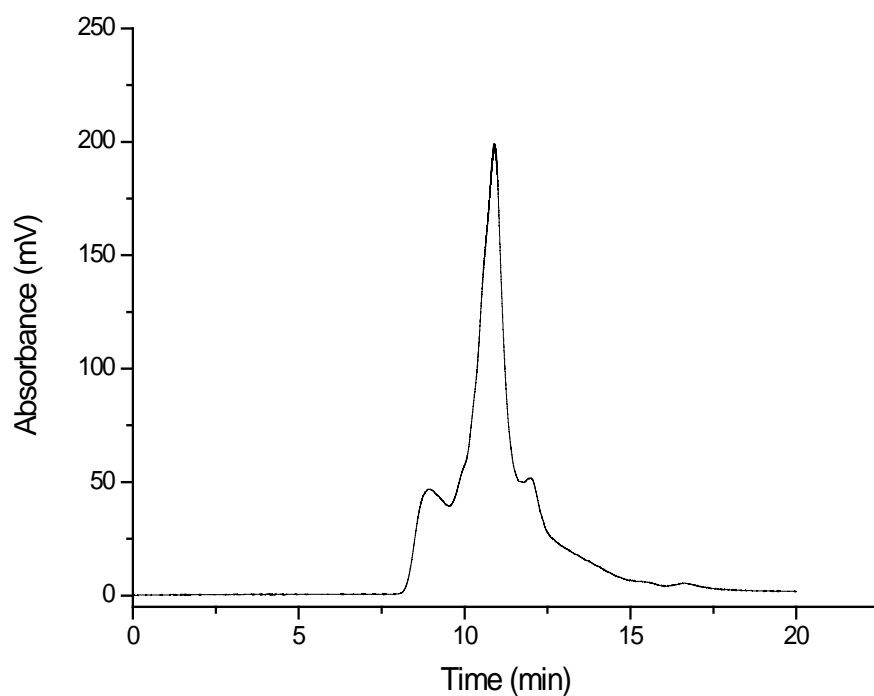


Figure 3.3 GPC data of gliadin extract

3.4 Conclusion

The purification of gliadin is a simple, productive, and efficient process, thanks to the easy access to commercial gluten. It's much easier to extract gliadin than hordein and kafirin. Gliadin protein is a complex group of wheat prolamins with varied molecular weight. The purity of the gliadin obtained was adequate to proceed with the gliadin nanoparticle study.

CHAPTER 4 STRUCTURE OF GLIADIN IN SOLUTION

4.1 Introduction

In order to better understand the prolamins in the delivery system—gliadin, it is essential to understand its conformation and size when dissolved in aqueous ethanol. The primary and secondary structure of gliadin have been well studied and understood. Glutamine and proline are two predominant amino acids in gliadin, and alpha-helices and reverse beta-sheets are present in all sub-types of gliadin proteins (Veraverbeke & Delcour, 2002).

Recently, research has been conducted on the assembly of glutenin via multi-angle static and dynamic light scattering, SAXS, and very small angle neutron scattering (VSANS) (Dahesh, Banc, Duri, Morel, & Ramos, 2014). Glutenin was observed as flexible polymer chains in a good solvent (50% aqueous ethanol). The same research group also concluded that glutenin behave distinctly in dilute and concentrated regimes, as branched polymer coils and polymeric gels, respectively (2014).

However, how gliadin protein is shaped in solution has not yet been studied before. In this thesis, 1 mg/ml gliadin in 60% aqueous ethanol is examined upon synchrotron small angle X-ray scattering (SAXS). SAXS is a fundamental tool in studying macromolecules. At low concentration (such as 1mg/ml), gliadin is well soluble in 50% to 75% aqueous ethanol. 60% ethanol was chosen, because gliadin in 60% ethanol was used in the finalized

formulation of this study.

4.2 Experimental method

SAXS measurement was conducted at Bio-CAT, 18-ID beam line section in Advanced Photon Source, Argonne National Laboratory. Gliadin was dissolved in 60% ethyl-ethanol at 1 mg/ml and filtered with 0.45 μ m membrane. 60% ethyl ethanol was also measured to get the background data. The X-ray wavelength was 1.033 Å. Image and data was generated by two cameras and a high-sensitivity CCD detector. A quartz capillary flow cell of 1.5 mm diameter was maintained at 25 °C and used as a sample holder. To load sample constantly and minimize radiation damage, a Microlab 500 Hamilton pump was used. Scattering data and fifteen curves were generated upon each measurement for further interpretation by GNOM software.

4.3 SAXS Results

Mathematical methods and modeling techniques are of great importance in SAXS data interpretation (Svergun *et al*, 2003). In this study, we used SAXS to determine the structural information of 1 mg/ml gliadin in 60% ethyl-ethanol solution. Therefore, analysis and model-fitting are based on isotropic and monodisperse system. The total scattering intensity, $I(Q)$, can be expressed as the following equation (Li *et al*, 2012).

$$I(Q) = n_p (\Delta\rho)^2 v^2 P(Q) S(Q)$$

In the equation above, n_p is the number of protein molecules in the solution; $\Delta\rho$ is the difference of electron densities between protein solution and the corresponding solvent; v is the specific volume of the protein, obtained from Fischer's empirical equation (Fischer *et al*, 2004); Q is the scattering factor determined by λ , the wavelength of the X-ray beam, and θ , the scattering angle; $Q=(4\pi/\lambda)\sin(\theta/2)$. $P(Q)$ is the form factor and related to protein conformation, and $S(Q)$ is the structure factor reflecting the aggregation behavior of the protein in a given solution (Li *et al*, 2012). Both $P(Q)$ and $S(Q)$ are expressed in empirical functions depending on the protein, protein concentration, and the solvent (Svergun *et al*, 2003).

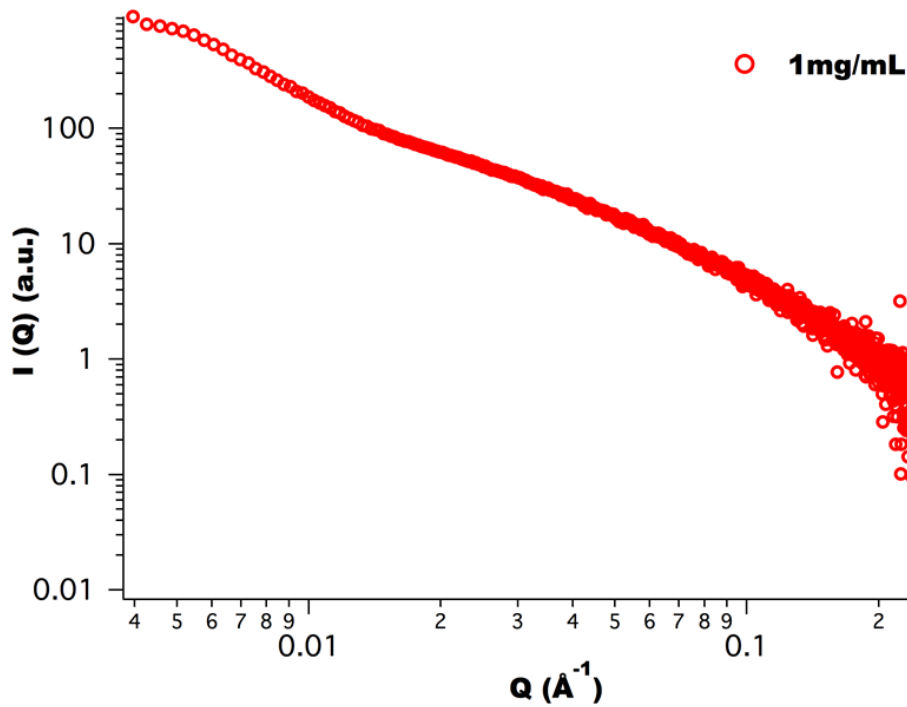


Figure 4.1 Intensity profile of 1mg/mL gliadin in 60% aqueous ethanol solution

In principle, the scattering intensity $I(Q)$ covers the same information as pair distribution function (PDF), yet PDF and Guinier plot are more intuitive and straightforward in fitting and predicting the shape of the protein of interest (Svergun *et al*, 2003). In other words, although the scattering intensity profile, or $I(Q)$, is a piece of fundamental and essential information in determining the assembly of macromolecules, the graph itself doesn't reveal any information directly. GNOM software or Guinier plot presents direct fitting upon different geometry models.

The Guinier plot delivers information on the radius of gyration(R_g), cross-section radius of gyration (R_c), or thickness (T), and PDF expresses size distribution (Svergun *et al*, 2003).

The Guinier approximation was given by the equation below.

$$I(Q) = \alpha \pi Q^{-\alpha} A \exp\left(-\frac{R_\alpha^2 Q^2}{3 - \alpha}\right)$$

In this equation, α is dependent on the shape of the protein: $\alpha = 0$ for solid sphere (also referred to as classic Guinier fit), $\alpha = 1$ for rod, and $\alpha = 2$ for sheet; A is the scattering intensity at $Q=0$ (Svergun *et al*, 2003). The value of R_g , R_c , and T can be obtained after the value of α , or the shape of the protein, is determined. To be specific, when $\alpha = 0$ (sphere), R_g equals R_α ; when $\alpha = 1$ (rod), R_c equals $\sqrt{2}R_\alpha$; when $\alpha = 2$ (sheet), T , the thickness, is equal to $\sqrt{12}R_\alpha$ (Svergun *et al*, 2003). GNOM package generated PDF or $P(r)$, which reveals the

distance distribution patterns of the protein body, thus determines the size of three dimensions (Semenyuk *et al*, 1991).

Fitting of gliadin protein against geometry models was completely based on the scattering intensity profile. Figure 4.2 and 4.3 illustrate the fitting of rod particle and globular particle, respectively. Other models such as ellipsoid rotation, cylinder, and hollow sphere were also tested (data not shown). Among the fittings with distinct geometry bodies, the model of ellipsoid demonstrated the best fit. Figure 4.4 shows the prolate ellipsoid fit of gliadin in 1 mg/ml solvent by GNOM (fitting points 50-500), and the dimensions were 157 Å~ 27 Å~ 6 Å.

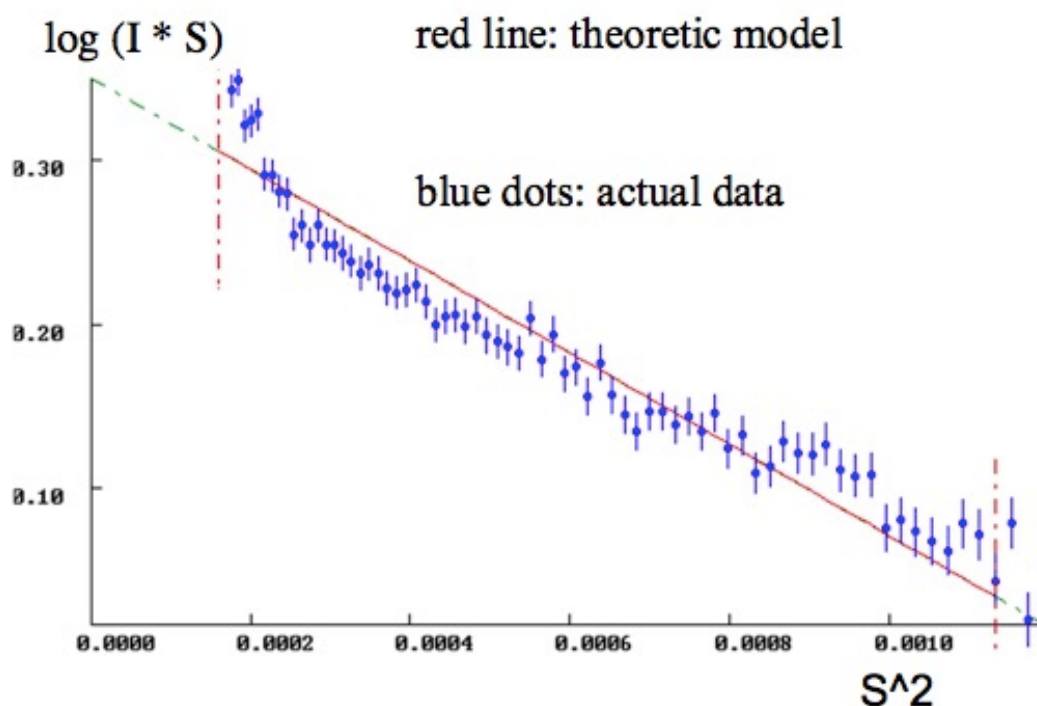


Figure 4.2 GNOM fitting for experimental data against model of rod

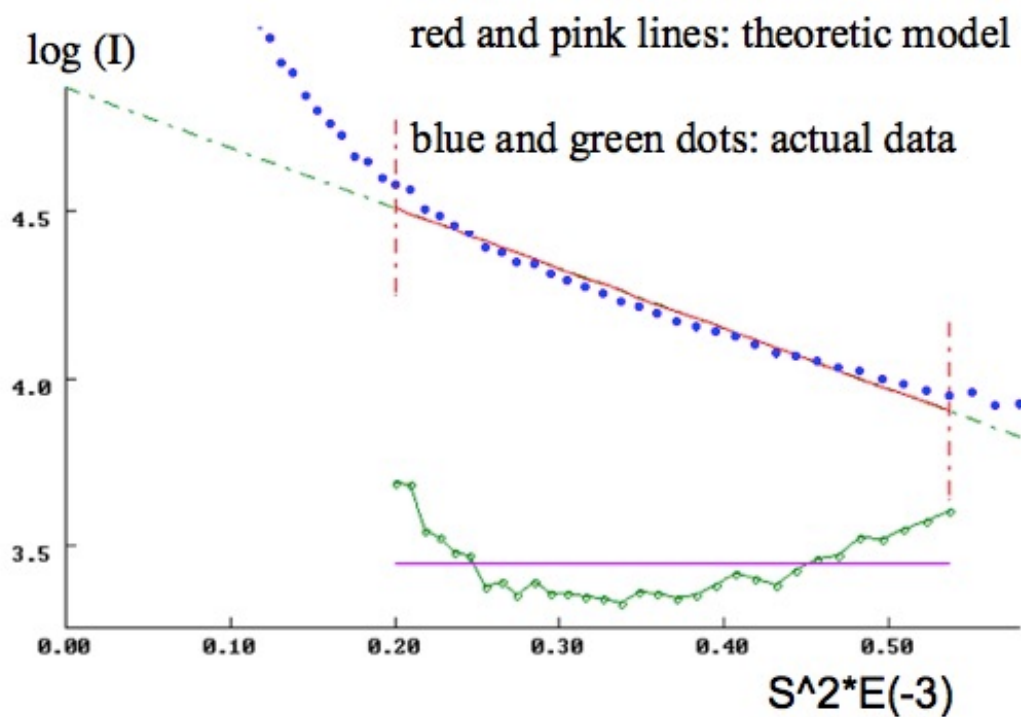


Figure 4.3 GNOM fitting for experimental data against model of globular

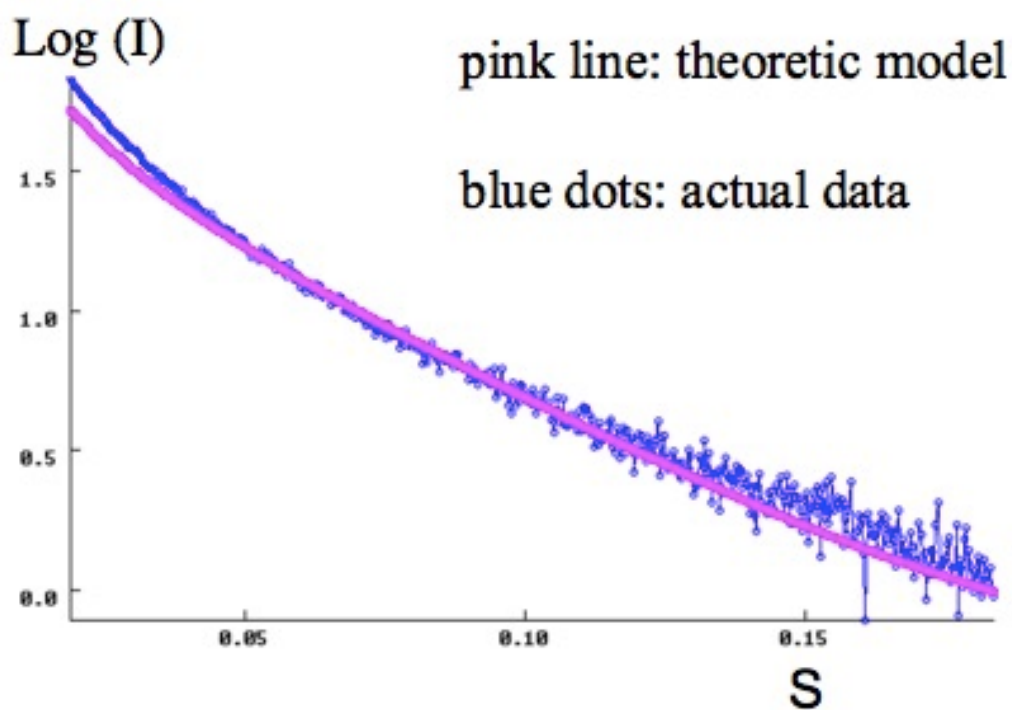


Figure 4.4 GNOM fitting for experimental data against model of prolate ellipsoid

4.4 Conclusion

To summarize, the extracted gliadin was dissolved in 60% aqueous ethanol and tested upon SAXS. Due to the absence of similar study on gliadin or its assembly and conformation, the data that could be compared with is extremely limited. So far, it is highly likely that gliadin is prolate ellipsoid in 60% ethanol.

CHAPTER 5 FORMULATION AND CHARACTERIZATION OF GLIADIN NANOPARTICLES

5.1 Introduction

Nanoparticles as delivery system has potential in controlled delivery and improving bioavailability of nutraceuticals. Prolamin-based nanoparticles are relatively easier to fabricate than other delivery system. Zein, kafirin, hordein, and gliadin are prolamins in corn/maize, sorghum, barley, and wheat. Those major cereals can be divided in two groups, temperate cereals and tropical cereals (Shewry & Tatham, 1990).

Among all the prolamins, zein has been well studied for its molecular structure, conformation, formulation of nanoparticles, cytotoxicity and cellular uptake properties. Others, however, are not well understood in terms of their conformation, application in delivery system, or cytotoxicity. Given that wheat is one of the most widely grown cereals, we focused on gliadin in this study.

In this chapter, the hydrophobicity of gliadin was tested and compared with other prolamins from major cereals. The favorable conditions for gliadin nanoparticle formation were carefully studied. To understand the potential application of gliadin nanoparticles in dietary supplements, the formulation was then used to load PMF. Physicochemical properties (such

as size, stability, morphology, and loaded efficiency) were measured for the PMF-loaded gliadin nanoparticles.

5.2 Materials and method

5.2.1 Materials

PMFs were extracted by our formal graduate students (purity > 95%) and used without further purification. Gliadin protein was extracted from commercial gluten (Vital Wheat Gluten) purchased from Arrowhead Mills. 60% ethyl-ethanol was prepared using 95% ethyl-ethanol from EMD Millipore. 200 proof ethanol and glacial acetic acid (ACS grade) were purchased from Sigma-Aldrich (Gillingham, UK). Water was purified by a Milli-Q system prior to use.

5.2.2 Fabrication of gliadin nanoparticles

Gliadin nanoparticles were prepared using anti-solvent induced precipitation method. Preliminary trails were conducted to determine the optimum conditions for stable nanoparticles without any non-food-grade chemical reagent. Conditions of particle fabrication include the concentration of gliadin solution, the ratio of solvent versus anti-solvent, and the presence of carboxyl-methyl chitosan (CMCS).

5.2.3 Hydrophobicity of gliadin

In order to compare the hydrophobicity of gliadin with other prolamins, the water-in-air

contact angle was measured. For preparation of homogeneous film, 10mg/ml gliadin in acetic acid solution was added onto a glass substrate. The glass substrate was then put into a circular spin coater under vacuum and left in ambient temperature for 30 min to dry. 2 μ L water was deposited onto gliadin film. Upon settling of the water droplet, the contact angle was detected by VCA optima setup (AST Products Inc., MA). Five measurements were taken on each film, and the gliadin film was prepared in triplicate.

5.2.4 Formulation of PMF loaded gliadin particles

Based on the preliminary trails, PMF (10 mg/ml) was dissolved in pure ethanol as a stock solution. Gliadin (15 mg/ml) was dissolved in 60% alcohol-aqueous solution. 52 μ L of PMF stock solution was added into 0.7 ml of gliadin solution in a dropwise manner under mechanical stir for 15 min. Then, the above gliadin-PMF solution was added drop by drop into 5 ml of water, the anti-solvent. The control/blank nanoparticles were prepared by replacing PMF stock solution with pure ethanol in parallel.

5.2.5 Morphological study by Atomic Force Microscopy (AFM)

20 μ L of freshly prepared blank and PMF loaded gliadin nanoparticles were dripped onto freshly cleaved mica surface separately after diluted with water/anti-solvent three times. After 30 mins' absorption, particles were washed with DI water and dried at 40 $^{\circ}$ C for 3h. AFM images using tapping mode were collected by NanoScope IIIA Multimode AFM

(Veeco Instruments Inc., Santa Barbara, CA).

5.2.6 Particle size distribution and ζ -potential measurement

Blank gliadin nanoparticles and PMF-gliadin nanoparticles were settled for 24 hours before size distribution and ζ -potential measurement. Particle size and size distribution were obtained by dynamic light scattering (DLS) using a BIC 90 Plus size analyzer with a Brookhaven BI-9000AT digital correlator (Brookhaven Instrument Corp., New York, NY). Measurements were made at a fixed scattering angle of 90 degree at 25 °C with a solid-state laser operating at 658nm. The polydispersity index (PDI) represented the distribution of particle size. The surface charge was measured by Delsa™ particle analyzer, Beckman Coulter. The surface charge was expressed by ζ -potential via Delsa™ Nano software. All measurements were performed in triplicate.

5.2.7 PMF loading and encapsulation efficiency in gliadin particles

Each batch of freeze-dried loaded nanoparticles was flushed with 5 ml ethyl acetate three times, using No.2 Whatman filter paper. The washed nanoparticles were dried in the fume hood and weighed. The ethyl acetate elute, which contained free PMF, was added 9 ml DMSO and dried under nitrogen atmosphere. A microplate reader (Molecular Devices, Sunnyvale, CA) at 326 nm was used to test the concentration of PMF in DMSO. To calculate loading and encapsulation efficiency, the equations were listed as following:

$$\text{Loading} = \frac{(W_{\text{total}} - W_{\text{free}})}{W_{\text{partilces}}} \times 100\%$$

$$\text{Encapsulation Efficiency} = \frac{W_{\text{total}} - W_{\text{free}}}{W_{\text{total}}} \times 100\%$$

Where W_{total} and W_{free} stand for the weight of PMF formulated in the system and the weight of free PMF washed out in ethyl acetate, respectively. $W_{\text{particles}}$ represents the weight of washed and dried nanoparticles.

5.3 Results and discussion

5.3.1 Optimum condition for gliadin nanoparticle formation

Nanoparticle formation is influenced by the ratio of solvent versus anti-solvent, prolamin concentration, ionic strength, and pH. Trails have been conducted in neutral pH and ionic strength as in DI water without any modification. Table 5.1 is a summary of particle size in different combinations of anti-solvent ratio and gliadin concentration; not all trails were shown. The diameters of nanoparticles have been rounded to tens digit.

Gliadin was dissolved in 60% ethanol. For trails with CMCS, CMCS was dissolved in anti-solvent, i.e., DI water, and gliadin solution was added into CMCS in water solution directly. Based on the trails, adding 0.7ml 15 mg/ml gliadin into 5 ml water yielded most stable particles. Generally, even and small particle size (around 100nm) indicates better stability. The addition of CMCS seemed to prevent particles from aggregation when gliadin was in high concentration. 0.7ml 15 mg/ml gliadin, 0.28ml 40 mg/ml, and 0.21ml 50mg/ml all

gave similar final gliadin concentration, yet their outcome differed.

Table 5.1 Trials of solvent vs. anti-solvent (Ratio v/v), gliadin concentration ([c] of gliadin), and presence of CMCS on particle size

[C] of gliadin: mg/ml	Ratio v/v	CMCS	Average diameter: nm
2.5	0.7:5	0	710
5	0.7:5	0	520
5	1.4:5	0	precipitate
5	1:5	0	720
10	0.7:5	0	precipitate
15	0.7:5	0	150
15	0.7:5	0.5mg/ml	360
15	0.7:5	1.5mg.ml	730
15	1.4:5	0	450
20	0.7:5	0	350
20	1:5	0	510
30	0.7:5	0	360
30	1:5	0	630
40	0.28:5	0	precipitate
40	0.7:5	0	precipitate

50	0.21:5	0	precipitate
50	0.21:5	0.5mg/ml	420
50	0.7:5	0	precipitate

5.3.2 Hydrophobicity of gliadin

On average, gliadin had a 44° water-in-air contact angle, demonstrated in Figure 5.1. Compared with zein (56°) and kafirin (72°), gliadin tends to be more hydrophilic (Xiao, Wang, Gonzalez, & Huang, 2016). On the other hand, gliadin shares similar hydrophobicity with hordein, which may be a result from their parallel amino acid profile (Shewry, Miflin, & Kasarda, 1984).

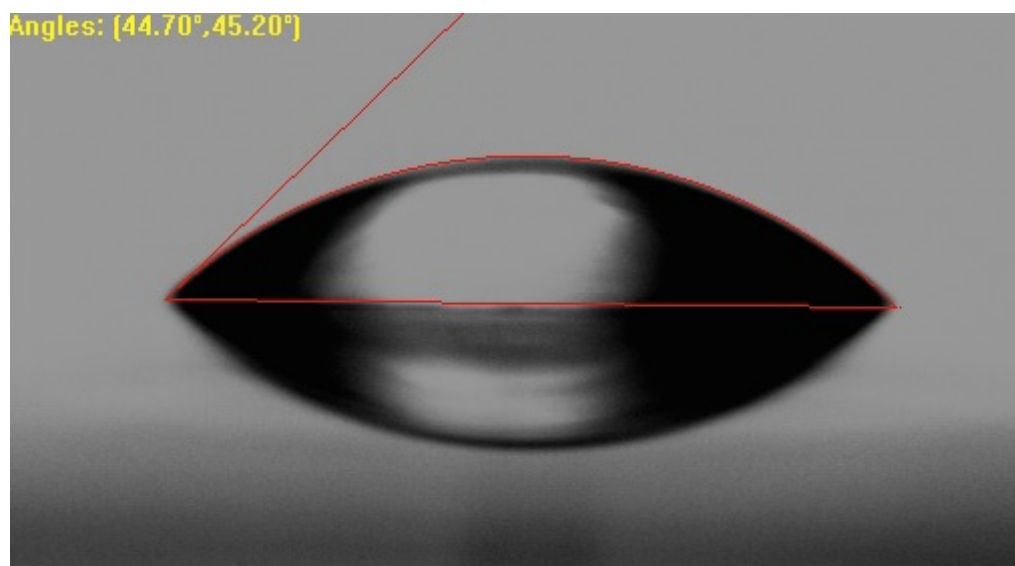


Figure 5.1 Water-in-air contact angle of gliadin film by VCA optima setup

Moreover, zein and kafirin are capable of forming stable nanoparticles when they are

dissolved in glacial acetic acid and induced by anti-solvent. Neither gliadin nor hordein is comparable to zein and kafirin in such aspect. When gliadin or hordein in acetic acid solution was added into water, the mixture is homogenous and clear; no particles were formed at all.

5.3.3 Morphology of PMF-loaded gliadin particle: AFM results

The morphological properties of individual or aggregated gliadin nanoparticles were revealed by AFM. Figure 5.2 and 5.3 were the height and 3D images, respectively, with blank gliadin nanoparticles on the left and PMF loaded gliadin particles on the right. Sphere-like particles were clearly observed in both images. The height reflected the diameter of the dried nanoparticles or particle aggregation indirectly. The decrease of particle size was expected, since protein shrinks after dehydration. Large dots indicated aggregations of nanoparticles due to drying.

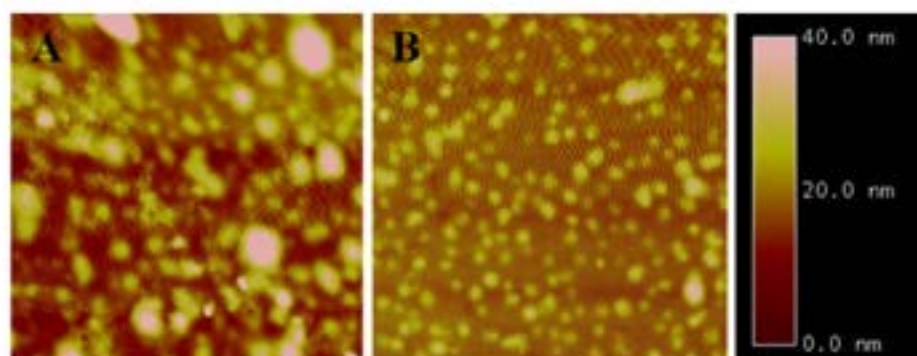


Figure 5.2 Height image of blank (left) and loaded (right) nanoparticles by AF

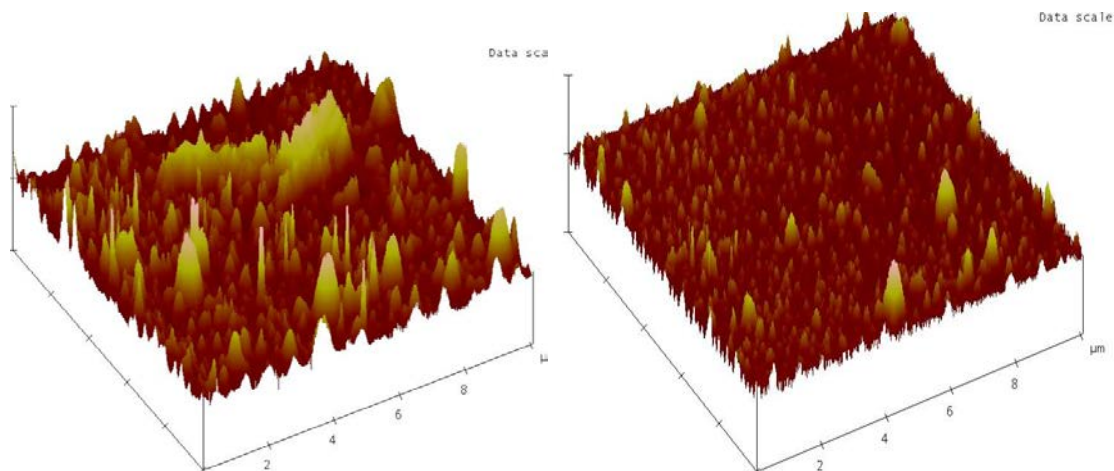


Figure 5.3 3-D image of blank (left) and loaded (right) nanoparticles by AFM

5.3.4 Physicochemical evaluation of gliadin nanoparticles

After the formulation of blank gliadin particles was defined, the concentration and volume of PMF stock solution was tested to maximize the loading of the system. Both blank gliadin and PMF loaded gliadin particles were milky, uniform suspensions (Figure 5.4). Characterization of the gliadin nanoparticles were reported (Table 5.2). The average size of loaded particles was 165.2 ± 1.9 nm, and a polydispersity index of 0.182 ± 0.008 demonstrated reasonable homogeneity, given that the materials (gliadin and PMFs) were derived from natural materials (gluten and orange peels).

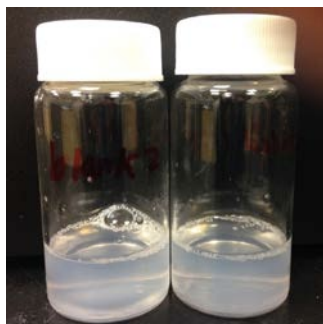


Figure 5.4 Direct observation of blank (left) and loaded (right) gliadin nanoparticles

The delivery system was relatively stable with no cross-linker or emulsifier, and had a zeta-potential of 13.35mV. Without abrupt change of pH or ionic strength, it takes months before the particles precipitate. It was also observed that the size of the particles had decreased slightly (by about 10%) after the evaporation of ethanol under nitrogen atmosphere. The absence or decrease in its good solvent probably induces the impulsion between gliadin particles. The loading and encapsulation efficiency of PMF loaded gliadin nanoparticles were 76% and 1.2%, respectively, leaving the effective PMF 92 µg/mL (approximately 242 µM/L; average MW 380 g/mol) in the system.

Table 5.2 Physicochemical properties of gliadin nanoparticles

Sample	Diameter/nm	PDI	ζ /mV	EE/%	Loading/%
Blank	147.8±5.8	.221±.017	11.01±0.60	--	--
Loaded	165.2±1.9	.182±.008	13.35±0.33	76	1.2

5.4 Conclusion

Gliadin-in-ethanol solution forms nanoparticles when induced by anti-solvent. Unlike kafirin or zein, gliadin couldn't form particles when dissolved in acetic acid. According to the water-in-air contact angle, the hydrophobicity of gliadin was similar to hordein and not so strong as zein or kafirin, which is probably related to biological classification. Major crops may be divided in two groups; barley and wheat belong to temperate cereals, and

maize and sorghum tropical cereals (Shewry & Tatham, 1990). Generally, greater hydrophobicity makes formation of nanoparticles easier. Given the large quantity of wheat production and simplicity of extraction process, gliadin is a fair candidate in formulating food delivery system.

The formulation of gliadin nanoparticles was defined and ready for use in further studies. Formed by self-assembly with no cross-linker, gliadin nanoparticles were stable and sized 150 nm, and dispersed water-insoluble nutraceuticals in aqueous system evenly. Particles were close to sphere, and had a reasonably loading and encapsulation efficiency.

CHAPTER 6 CYTOTOXICITY OF GLIADIN PARTICLE FORMULATION AND ITS CELLULAR UPTAKE PROFILE

6.1 Introduction

Gliadin is part of natural cereal, and has been consumed by human for hundreds of years. Gliadin, when in its native form, is GRAS. However, the cytotoxicity of gliadin nanoparticles is largely unknown. In order to better understand gliadin nanoparticles as a delivery system, cell viability and cellular uptake studies have been conducted on Caco-2 colon carcinoma cell lines, the widely accepted and used cell model for cytotoxicity in food science.

The MTT (3-(4,5-dimethylthiazol-2-yl)-2,5-diphenyltetrazolium bromide) tetrazolium reduction assay was carried out on raw PMF, blank gliadin nanoparticles, and PMF-loaded gliadin nanoparticles. The concentration of PMF was expressed in $\mu\text{g/mL}$, and an estimate of $\mu\text{M/L}$ was given based on the average molecular weight of PMFs. 90% cell viability was used as a boundary as of cytotoxicity. The formulation was diluted till it would be considered “non-cytotoxic”, and then examined on cellular uptake test.

6.2 Materials and methods

6.2.1 Materials

Caco-2 cell line was generously provided by Department of Biology at Rutgers. Dulbecco's

modified Eagle medium (DMEM), fetal bovine serum (FBS), 100 unites/ml penicillin, streptomycin and ethylene-diaminetetraacetic acid (EDTA) were all purchased from Fisher Scientific. Dimethyl sulfoxide (DMSO) was purchased from Sigma (St. Louis, MO). The final concentration of DMSO is 0.1% or lower in the media. The results were measured upon Synergy HT multimode microplate reader (BioTek Instruments, Winooski, VT).

6.2.2 Cytotoxicity of raw PMFs, blank gliadin particles, and PMF-loaded gliadin particles

Caco-2 colon carcinoma cells were cultured in Dulbecco's modified Eagle's medium (DMEM) with 10% fetal bovine serum (FBS), 100U/ml penicillin G, 0.1mg/ml streptomycin, and 1% minimum essential medium (MEM) non-essential amino acid solution. The incubator used provided a 5% CO₂ atmosphere at 37 °C. Caco-2 cells were seeded at 10000 cells per well in 96 well plate in 100µL media.

After 24h, raw PMF in DMSO was added to the cells with a series of concentrations (5, 10, 25, 50, 60, 70, 80, 90, 100 µg/mL media; equivalent to 13, 26, 66, 132, 158, 184, 210, 237, and 263 µM PMFs/L media). Untreated cells function as control group. After 24h, media were aspirated, and cells were settled in 100µL MTT solution for 4h. DMSO was then added to dissolve the formazan crystals, and the optical density was measured under 570nm using BioTek Synergy HT multimode microplate reader. Each sample was conducted in

triplicates. Cell viability was calculated as

$$\text{Viability} = \frac{N_t}{N_c} \times 100\%,$$

Where N_t is the optical density of cells treated and N_c the untreated/control cells.

Similar procedure was carried out to test the cytotoxicity of blank and loaded gliadin nanoparticles. Briefly, freshly prepared blank gliadin nanoparticles was diluted with cell media for a series of concentration (1.84, 0.92, 0.46, 0.23, 0.12, 0.058, 0.029, 0.014, and 0.072 mg gliadin/ml media). The same diluting series of PMF loaded nanoparticles were prepared. A parallel series of free PMF equivalent to the PMF concentration in loaded nanoparticles was the positive control of the experiment (46, 23, 12, 5.8, 2.9, 1.4, 0.72, 0.36, and 0.18 μg PMF/mL media, equivalent to 121, 60, 32, 15, 8, 3.7, 2, 1, 0.5 μM PMFs/L media).

6.2.3 Statistical analysis

Cytotoxicity of blank gliadin nanoparticle system were examined upon one-way ANOVA using OriginPro 8. All the experiments were performed in triplicate at least, and error bars in the figures represent standard deviation.

6.2.4 Cellular uptake study on PMF-loaded gliadin nanoparticles

Qualitative cellular uptake study was conducted on PMF-loaded gliadin particles. Caco-2

cells were seeded in Multiwell™ 12-well Tissue Culture Plates (Falcon®, BD Biosciences, NJ). The cells were cultured in a cell culture incubator (NAPCO 5400, Fisher Scientific, PA) at 37°C for 12 h. Encapsulated during nanoparticle formation, coumarin 6 was used as a fluorescent marker. The cells were treated with diluted PMF-loaded gliadin nanoparticles (23 µg PMF/mL media), since the cytotoxicity study suggested such dose should show little, if there is any, cytotoxicity. At certain time intervals (0, 0.5, 1, 2, 4, and 8h), the 12-well culture plates were removed from incubator. To make sure there was no residue of nanoparticles, the monolayer of Caco-2 cells was rinsed with 1 ml PBS (0.01M, pH7.4). After that, Dulbecco's phosphate buffered saline was added to the cells. The fluorescent intensity was viewed by fluorescence microscopy and recorded as photos by Nikon Eclipse TE2000-U.

6.3 Results and discussion

6.3.1 Cell viability of raw PMFs, blank gliadin particles, and PMF-loaded gliadin particles

Figure 6.1 demonstrated the cytotoxicity of raw PMFs in DMSO on Caco-2 cells. Below 25 µg/mL (65.85µM/L), little cytotoxicity was reported. When the concentration of PMFs increased beyond 50 µg/mL (131.5µM/L), PMF showed significant cytotoxicity on Caco-2 cells. The original PMF loaded nanoparticles had 92 µg/mL (242 µM/L), and an effective dose around 70 µg/mL (184 µM/L) considering the encapsulation efficiency.

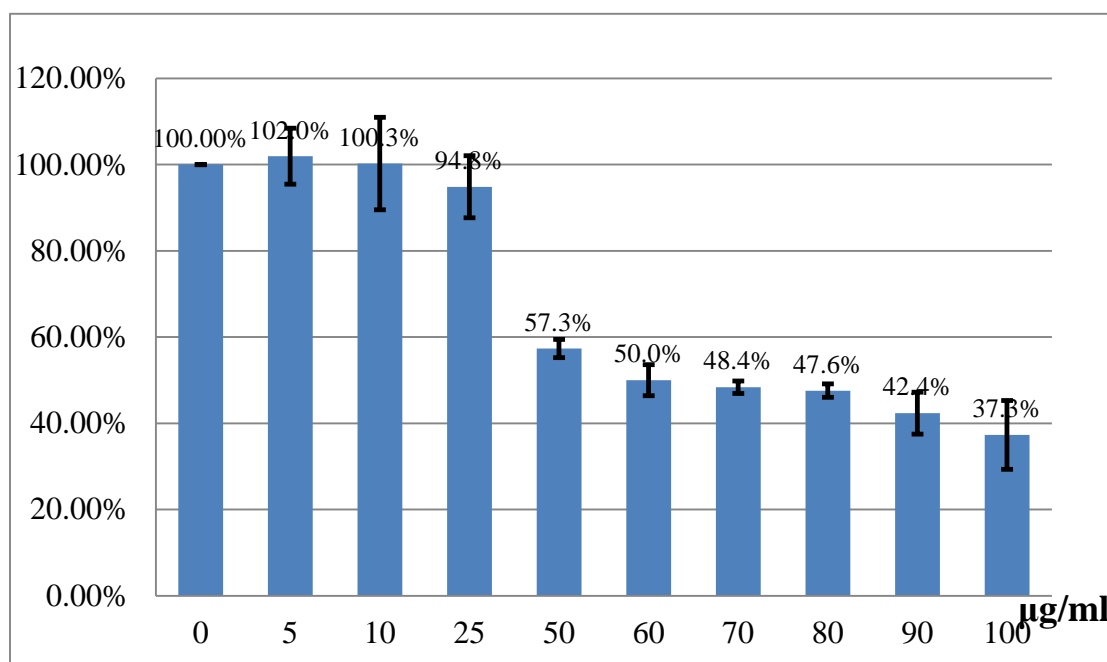


Figure 6.1 Cell viability of Caco-2 cells treated with PMF in DMSO

The cytotoxicity of the blank gliadin nanoparticles system was also studied. The formulation was tested when it was fresh and in original condition as nanoparticle suspension, with no further modification. After a series of half dilution, the samples were added in to the media, with the highest concentration (1.84 mg gliadin/mL media) as half of the original formulation. The result (Figure 6.2) suggested that all the concentration treatments gave out a 93% or higher cell viability, meaning that none of the above concentration reflects cytotoxicity. Further statistic analysis (one-way ANOVA) confirms that neither concentration treatment was significantly different from the control group ($p < 0.05$). Therefore, the gliadin nanoparticle formulation had little (if there is any) cytotoxicity in its original form or any of its dilutions.

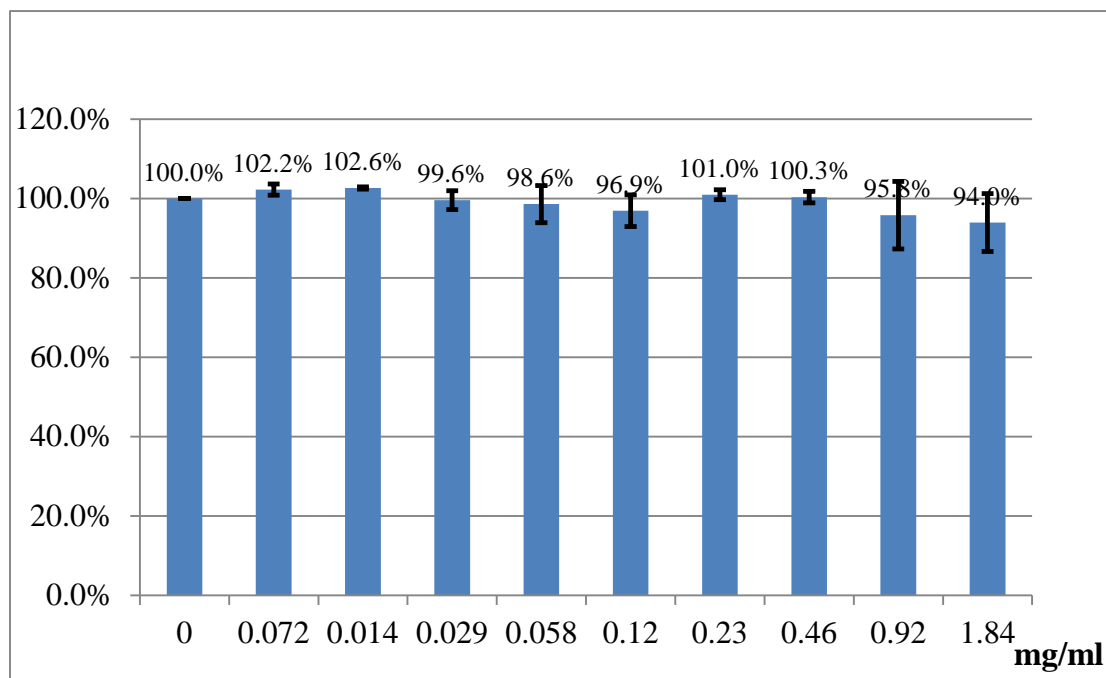


Figure 6.2 Cell viability of Caco-2 cells treated with a series dilution

The second step is to examine the cytotoxicity of PMF-loaded nanoparticles. The loaded formulation was diluted exactly the same way as the blank nanoparticles, and a corresponding series of raw PMF in DMSO was examined in parallel, with concentration treatments the same as the loaded formulation. As shown in Figure 6.3, cell viability of the group of PMF loaded particles is concentration dependent. When the original formulation was diluted four times or more (from the second right bar to the left), the cytotoxicity was minimum. Also, the result of cells treated with raw PMF was similar to that in the previous section (cytotoxicity of raw PMFs), thereby reinforcing the results in Figure 6.1. Comparing the test group and the positive control group, the cell viability was higher when PMF was loaded in gliadin particles than in DMSO. To sum up, PMF-loaded formulation

has little cytotoxicity after four-time dilution or more.

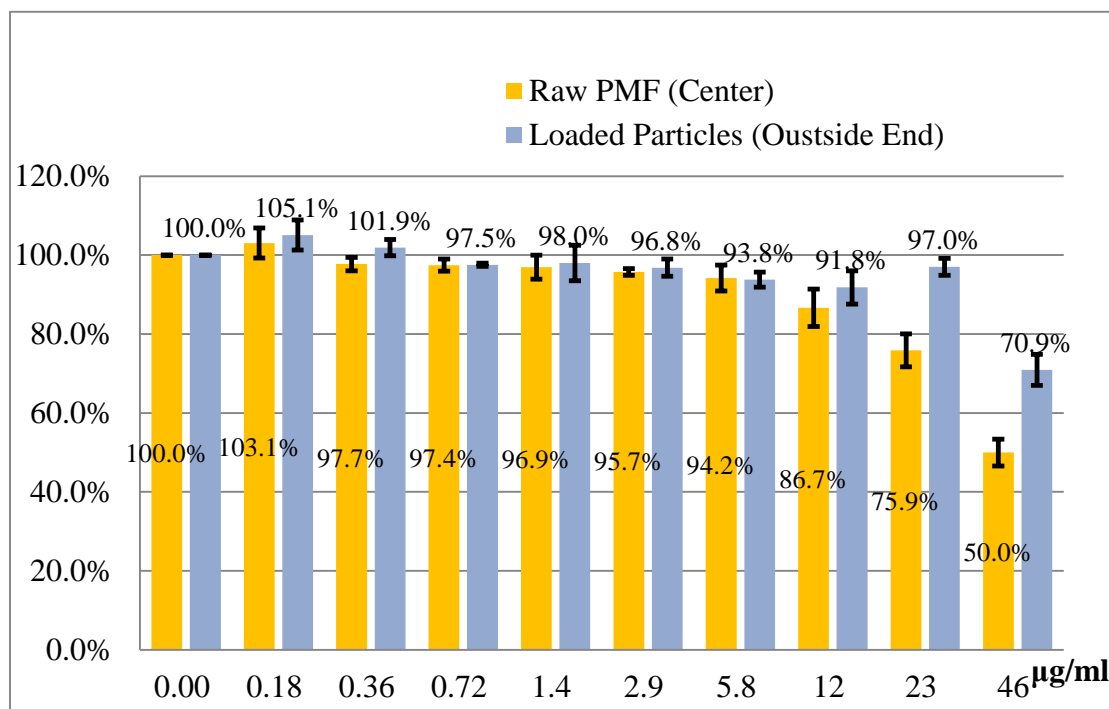


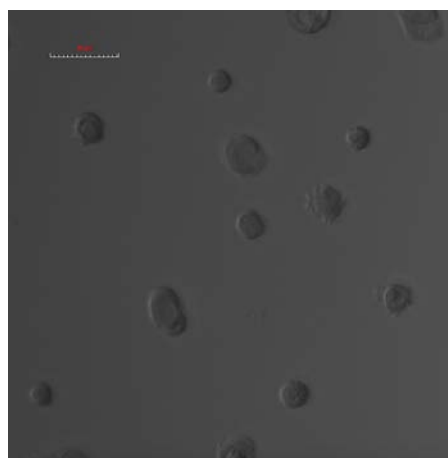
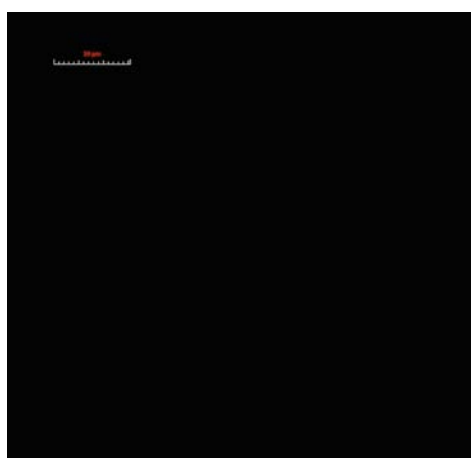
Figure 6.3 Cell viability of Caco-2 cells treated with PMF in DMSO and PMF-loaded nanoparticles

6.3.2 Cellular uptake profile of final formulation

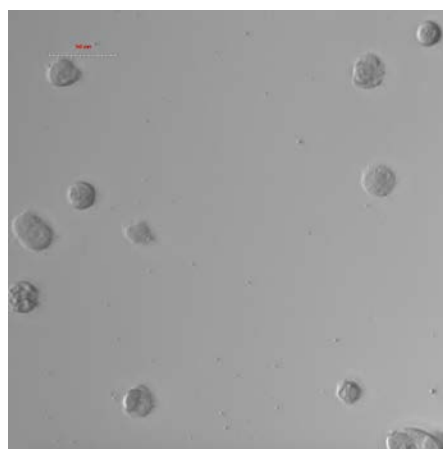
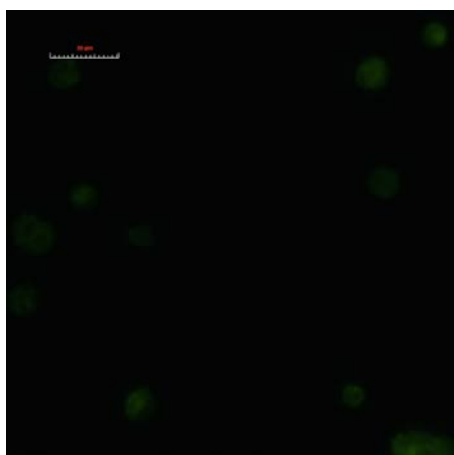
Figure 6.4 illustrated the cellular uptake profile of loaded nanoparticles. Coumarin 6 was chosen as the fluorescence marker, because coumarin 6 is lipophilic and dyes gliadin not aqueous phase (Zhang & Feng, 2006). Therefore, the fluorescence signal in the Figure 6.4 was a truly indicative of particle or aggregated particle absorbed by cells.

Based on Figure 6.4, gliadin nanoparticle could be absorbed by Caco-2 cells. The signal of fluorescence increased steadily during the trial, suggesting a time dependent behavior in

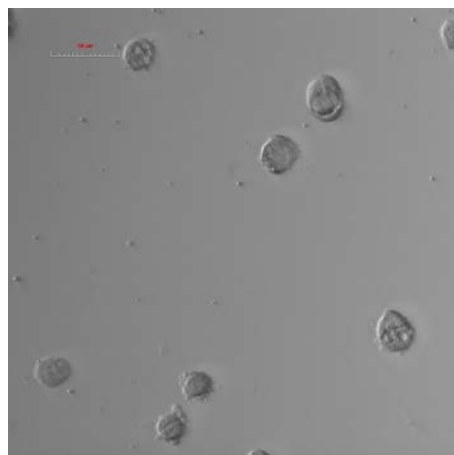
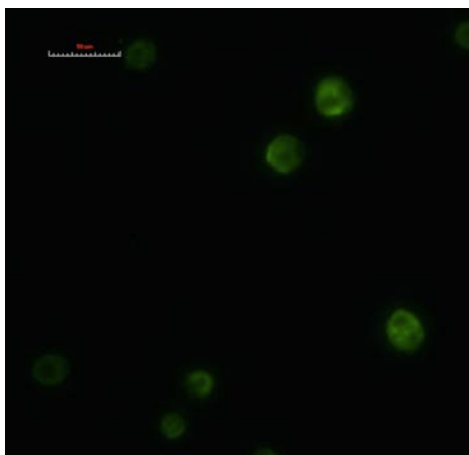
terms of cellular uptake. Such increase was most significant between 0.5 to 4h. Given the average particle size, it was highly unlikely that particles were transported through paracellular pathway (Li, Jiang, Xu, & Gu, 2015). Instead, enterocytes might have been the major route for the uptake of gliadin particles. Left column were fluorescence photos, while right column were optical ones.



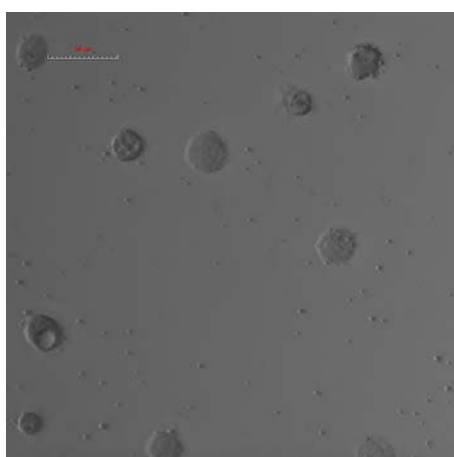
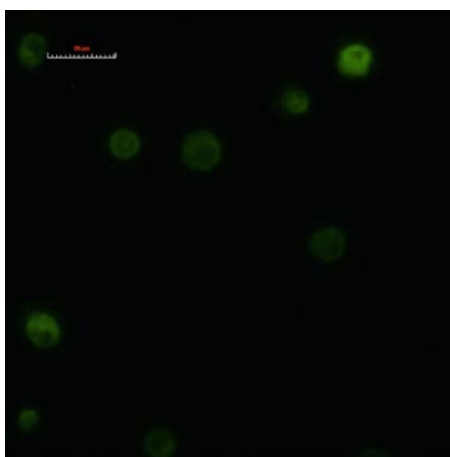
0h



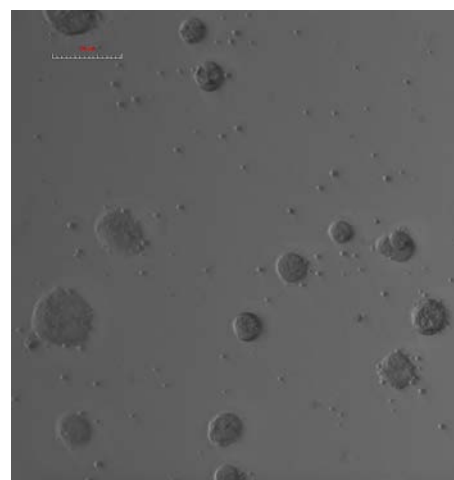
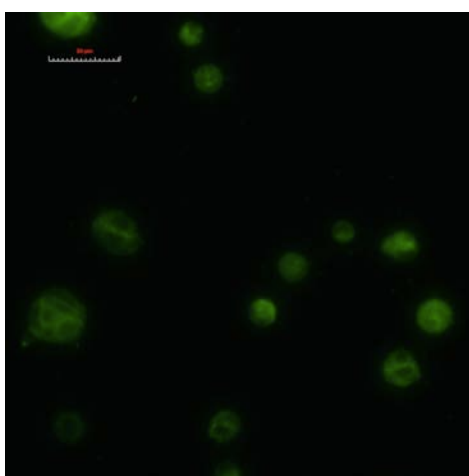
0.5h



1h



2h



4h

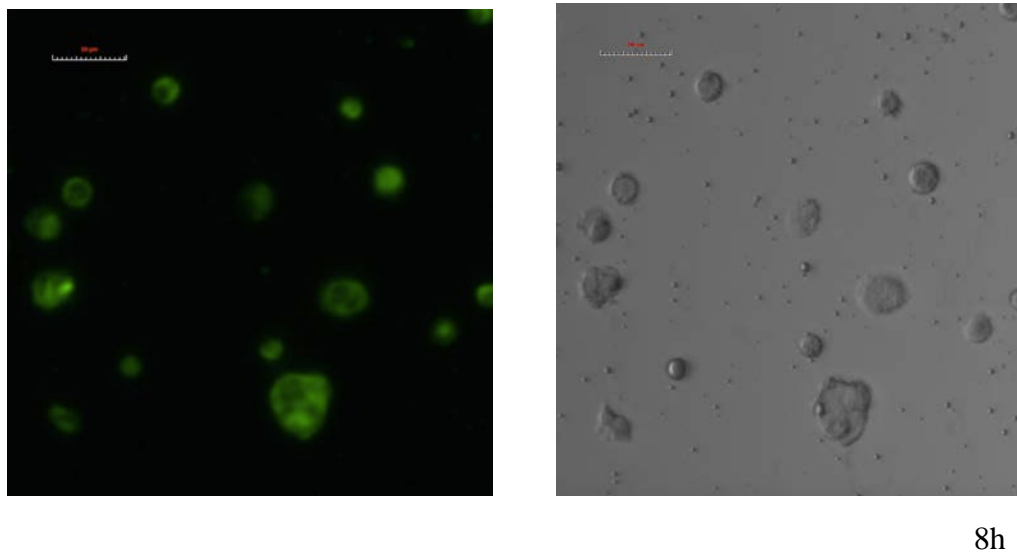


Figure 6.4 Cellular uptake of final formulation: fluorescence

6.4 Conclusion

Gliadin nanoparticle system had little or no cytotoxicity on Caco-2 cells. Raw PMF in DMSO had negligible cytotoxicity only when its concentration is 25 $\mu\text{g/ml}$ (66 $\mu\text{M/L}$) or below. The PMF-loaded gliadin particles showed no significant toxicity on or beyond four-time dilution. The cellular uptake of the final formulation was time dependent, and was probably through enterocytes.

REFERENCES

1. Balaguer, M., Cerisuelo, J., Gavara, R., & Hernandez-Muñoz, P. (2013). Mass transport properties of gliadin films: Effect of cross-linking degree, relative humidity, and temperature. *Journal Of Membrane Science*, 42, 380-392.
2. Bell, L.N. (2001). Stability Testing of Nutraceuticals and Functional Foods. *Handbook of Nutraceuticals and Functional Foods*, 501-516.
3. Bendedouch, D., Chen, S. H. (1983). Study of intermicellar interaction and structure by small angle neutron scattering. *J. Phys. Chem. B*, 87, 1653-1658.
4. Breinholt, V., Rasmussen, S., Brosen, K., Friedberg, T. (2003). In vitro metabolism of genistein and tangeretin by human and murine cytochrome P450s. *Pharmacology & Toxicology*, 93, 14-22.
5. Couvreur, P., Dubernet, C., & Puisieux, F. (1995). Controlled drug delivery with nanoparticles : current possibilities and future trends. *European journal of pharmaceutics and biopharmaceutics*, 41(1), 2-13.
6. Dahesh, M., Banc, A., Duri, A., Morel, M.H., & Ramos, L. (2014). Polymeric assembly of gluten proteins in an aqueous ethanol. *The Journal of Physical Chemistry B*, 118, 11065-11076.
7. Damodaran, S., Parkin, K., Fennema, O. (2007). *Food chemistry* (4th ed.). CRC Press.
8. Delcour, J., Joye, I., Pareyt, B., Wilderjans, E., Brijs, K., & Lagrain, B. (2012). Wheat Gluten Functionality as a Quality Determinant in Cereal-Based Food Products. *Annual Review Of Food Science And Technology*, 3, 3469-492.
9. Don, C., Lichtendonk, W., Plijter, J.J., & Hamer, R.J. (2003). *Glutenin macropolymer: a gel formed by glutenin particle*. *Journal of Cereal Science*, 37, 1-7.
10. Duclairoir, C. C., Orecchioni, A. M., Depraetere, P. P., & Nakache, E. E. (2003). Evaluation of gliadins nanoparticles as drug delivery systems: a study of three different drugs. *International Journal Of Pharmaceutics*, 253, 133-144.
11. Elzoghby A, Abo El-Fotoh W, Elgindy N. (2011). Casein-based Formulations as Promising Controlled Release Drug Delivery Systems. *Journal of Controlled Release*, 153 (3), 206-216.

12. Ezpeleta, I., Irache, J. M., Stainmesse, S., Chabenat, C., Gueguen, J., Popineau, Y., & Orecchioni, A. (1996). Gliadin Nanoparticles for the Controlled Release of all-Trans-Retinoic acid. *International Journal of Pharmaceutics*, 131(2), 191-200.
13. FAOSTAT. (2011). *Database of World Agriculture*. <http://www.faostat.org>
14. Galindo-Rodriguez, S.A., Allemann, E., Fessi, H., & Doelker, E. (2005). Polymer Nanoparticles for Oral Delivery of Drugs and Vaccines: a Critical Evaluation of *in Vivo* Studies. *Critical ReviewsTM in Therapeutic Drug Carrier Systems*, 22(5), 419-464.
15. Ho, C., Pan, M., Lai, C., Li, S. (2012). Polymethoxyflavones as food factors for the management of inflammatory diseases. *Journal of Food and Drug Analysis*, 20 (1), 337-341.
16. Huang, Q. R., Dubin, P. L., Lal, J., Moorefield, C. N., Newkome, G. R. (2005). Small-angle neutron scattering studies of charged carboxyl-terminated dendrimers in solutions. *Langmuir*, 21, 2737-2742.
17. Joye, I., Nelis, V., & McClements, D.J. (2015). Gliadin-based nanoparticles: fabrication and stability of food-grade colloidal delivery systems. *Food Hydrocolloids*, 44, 86-93.
18. Kalra, E.K. (2003). [Nutraceutical-definition and introduction](#). *AAPS pharmSci*, 5 (3), 27-28.
19. Kieffer, R. R., Schurer, F. F., Köhler, P. P., & Wieser, H. H. (2007). Effect of hydrostatic pressure and temperature on the chemical and functional properties of wheat gluten: Studies on gluten, gliadin and glutenin. *Journal Of Cereal Science*, 45(3), 285-292
20. Kobrehel, K., Bois, J., & Falmet, Y. (1991). A comparative analysis of the sulfur-rich proteins of durum and bread wheats: their possible functional properties. *Cereal Chemistry*, 68, 1-6.
21. Koehler, P. P., Kieffer, R. R., & Wieser, H. H. (2010). Effect of hydrostatic pressure and temperature on the chemical and functional properties of wheat gluten III. Studies on gluten films. *Journal Of Cereal Science*, 51(1), 140-145.
22. Kurowska, E., Manthey, J. (2004). Hypolipidemic effects and absorption of citrus

- polymethoxylated flavones in hamsters with diet-induced hypercholesterolemia. *Journal of Agriculture and Food Chemistry*, 52, 2879-2886.
23. Lagrain, B., Brijs, K., Veraverbeke, W.S., & Delcour, J.A. (2005). The impact of heating and cooling on the physico-chemical properties of wheat gluten-water suspensions. *Journal of Cereal Science*, 42(3), 327-333.
 24. Lamprecht A, Saumet J, Roux J, Benoit J. (2004). Lipid Nanocarriers as Drug Delivery System for Ibuprofen in Pain Treatment. *International Journal of Pharmaceutics*, 278(2):407-414.
 25. Li, S., Lambros, T., Wang, Z., Goodnow, R., Ho, C. (2007). Efficient and scalable method in isolation of polymethoxyflavones from Orange peel extract by supercritical fluid chromatography. *Journal of Chromatography B*, 846, 291-297.
 26. Li, S., Pan, M., Lo, C., Tan, D., Wang, Y., Shahidi, F., & Ho, C. (2009). Chemistry and health effects of polymethoxyflavones and hydroxylated polymethoxyflavones. *Journal Of Functional Foods*, 1, 2-12.
 27. Mintel Report (2014). Vitamins, Minerals, and Supplements: US September 2014.
 28. Miyata, Y., Sato, T., Imada, K., Dobashi, A., Yano, M., Ito, A. (2008). A citrus polymethoxyflavonoid, nobiletin, is a novel MEK inhibitor that exhibits antitumor metastasis in human fibrosarcoma HT-1080 cells. *Biochemical and Biophysical Research Communications*, 336, 168-173.
 29. Morley, K., Ferguson, P., & Koropatnick, J. (2007). Tangeretin and nobiletin induce G1 cell cycle arrest but not apoptosis in human breast and colon cancer cells. *Cancer Lett*, 251 (1), 168-78.
 30. Nielsen, S., Breinholt, V., Cornett, C., & Dragsted, L. (2000). Research Section: Biotransformation of the citrus flavone tangeretin in rats. Identification of metabolites with intact flavane nucleus. *Food and Chemical Toxicology*, 38(9), 739-746.
 31. Osborne, T.B. (1907). *The proteins of the wheat kernel*. Washington D.C.: Carnegie Institute.
 32. Pintore, M., Piclin, N., Chrétien, J., & Van De Waterbeemd, H. (2003). Prediction of oral bioavailability by adaptive fuzzy partitioning. *European Journal Of Medicinal Chemistry*, 38(4), 427-431

33. Shewry, P.R., Mifflin, B.J., & Kasarda, D.D. (1984). The structural and evolutionary relationships of prolamins storage proteins of barley, rye, and wheat. *Philosophical transactions of the Royal Society of London. Series B, Biological Sciences*, 304, 297-308.
34. Shewry, P.R. & Tatham, A.S. (1990). The prolamins storage proteins of cereal seeds: structure and evolution. *Biochemistry Journal*, 267, 1-12.
35. Singh, H., & MacRitchie, F. (2001). Application of polymer science to properties of gluten. *Journal of Cereal Science*, 33, 231-43.
36. Stoner, G., Naito, Z., You, M., Galati, A., Bowman, D., Resau, J., & Harris, C. (1991). Establishment and characterization of SV40 T-antigen immortalized human esophageal epithelial cells. *Cancer Research*, 51(1), 365-371.
37. Svergun, D. I. (1999). Restoring low resolution structure of biological macromolecules from solution scattering using simulated annealing. *Biophys. J.* 76, 2879-2886.
38. Svergun, D. I.; Koch, M. H. J. (2003). Small-angle scattering studies of biological macromolecules in solution. *Rep. Prog. Phys*, 66, 1735-1782.
39. Tatham, A.S., Masson, P., & Popineau, Y. (1990). Conformation studies of peptides derived by the enzymic-hydrolysis of a gamma-type gliadin. *Journal of Cereal Sciences*, 11, 1-13.
40. Ting, Y., Xia, Q., Li, S., Ho, C., & Huang, Q. (2013). Design of high-loading and high-stability viscoelastic emulsions for polymethoxyflavones. *Food Research International*, 54, 633-640.
41. Veraverbeke, W.S., & Delcour, J.A. (2002). Wheat protein composition and properties of wheat glutenin in relation to breadmaking functionality. *Critical Reviews in Food Science and Nutrition*, 42, 179-208.
42. Wang, P, Chen, H, Mohanad, B, Xu, L, Ning, Y, Xu, J, Wu, F, Yang, N, Jin, Z, & Xu, X. (2014). Effect of frozen storage on physico-chemistry of wheat gluten proteins: Studies on gluten-, glutenin- and gliadin-rich fractions'. *Food Hydrocolloids*, 39, 187-194.
43. Wieser, H. (2007). Chemistry of Gluten Proteins. *Food Microbiology*, 24(2), 115-119.
44. Wieser, H., Antes, S., & Seilmeier, W. (1998). Quantitative determination of gluten

- protein types in wheat flour by reserved-phase HPLC. *Cereal Chemistry*, 75(5), 644-650.
45. Xiao, J., Wang, X., Gonzalez, A.J., & Huang, Q. (2016). Kafirin nanoparticles-stabilized Pickering emulsions: microstructure and rheological behavior. *Food Hydrocolloids*, 54, 30-39.
46. Zhang, Z., Feng, S.S. (2006) The drug encapsulation efficiency, in vitro drug release, cellular uptake and cytotoxicity of paclitaxel-loaded poly (lactide)-tocopheryl polyethylene glycol succinate nanoparticles. *Biomaterials*, 27, 4025-4033.